J. Phys. Chem. A **2004,** *108,* 97−106

Theoretical Study of 1,3,4,6,7,9,9b-Heptaazaphenalene and Its Ten Derivatives

Wenxu Zheng,[†] Ning-Bew Wong,*[,‡] Weizhou Wang,[†] Ge Zhou,[†] and Anmin Tian*[,†]

Faculty of Chemistry, Sichuan University, Chengdu 610064, People's Republic of China, and Department of Biology and Chemistry, City University of Hong Kong, Kowloon, Hong Kong

Received: June 3, 2003; In Final Form: September 23, 2003

Density functional theory has been used to study the geometries, electronic structures, harmonic vibrational frequencies, and high-energy density material properties of 1,3,4,6,7,9,9b-heptaazaphenalene and its 10 derivatives (2,5,8-triR-1,3,4,6,7,9,9b-heptaazaphenalene, R = NH_2, OH, N_3, NO_2, F, Cl, Br, $-C{\equiv}N$, $-CH{=}CH_2$, and $-C{\equiv}CH$) at the B3LYP/aug-cc-pVDZ level of theory. Geometry studies show that all of the compounds have a highly symmetric structure with a planar and rigid heteroring. Calculation results confirm that there exists considerable conjugation over the parent ring, which is an advantage to the stabilities of these compounds. Substituent effects on the geometry, electronic structure, conjugation, HOMO, and LUMO of the parent ring are discussed in detail. Vibrational frequency studies indicate that the parent ring has a characteristic frequency and the substitution of all of the substituents makes it shift to a lower wavenumber. Moreover, our study shows that some of our discussed compounds may be potential candidates for high-energy density materials (HEDMs).

1. Introduction

The azabenzenes are important parent molecular systems for numerous compounds such as the biologically active nicotinic acid or the nucleotides cytosine, uracil, and thymine.[1,2] Especially, 1,3,5-triazine-based chemicals (usually abbreviated as s-triazine) have found various applications in manufacture of polymers, dyes, explosives, pesticides, and commodity chemicals.[3] These s-triazine monocyclic systems have been subjected to theoretical and experimental studies, and they are known as an obviously important set of conjugated heterocycles the electronic properties of which are expected to show subtle differences from those of benzene because of the successive replacement of CH groups by nitrogen atoms. Some researchers have indicated that the formation of molecular complexes (e.g., di-, tri-, oligo-, and polymers) is a conceivable way to increase density and stability and to improve the material properties of chemicals,[4] so we are interested in the performance of 1,3,4,6,7,9,9b-heptaazaphenalene-based chemicals composed of three s-triazines. In 2000, 2-azido-5,8-dihydroxy-1,3,4,6,7,9,9b-heptaazaphenalene was reported as a mystery molecule in the *Chemical & Engineering News*.[5] This molecule was preserved on Linus Pauling's office chalkboard, as it was just before he died in 1994. However, its function and why Pauling was interested in it is unknown. In fact, in the 1830s, a group of related nitrogen compounds, melem, hydromelonic acid, cyameluric chloride, cyameluric acid, etc., were known that possessed high heat stability, low solubility, and little chemical reactivity.[6,7] However, because of their insolubility and chemical inertness, these compounds remained structural puzzles for more than a century. In 1937, Pauling and Sturdivant[8] suggested a formulation for their common nucleus, a coplanar arrangement of three fused s-triazine rings. In the past decades, only one 1,3,4,6,7,9,9b-heptaazaphenalene-based compound was studied in detail, namely, the molecule 1,3,4,6,7,9,9b-heptaazaphenalene, $C_6N_7H_3$. Its structural and spectroscopic properties including an X-ray crystal structure analysis were discussed. UV photoelectron spectra were taken and ab initio calculations performed to explain the low basicity and the high stability.[9−12] In 2002, Kroke et al. reported the synthesis and detailed structural characterization of a functionalized 1,3,4,6,7,9,9b-heptaazaphenalene derivative, 2,5,8-trichloro-1,3,4,6,7,9,9b-heptaazaphenalene.[13] To our knowledge, other compounds containing the 1,3,4,6,7,9,9b-heptaazaphenalene unit have been only briefly mentioned in communications or patents and were not characterized at all.

The aim of our work is to study the geometric and electronic structures and properties of 1,3,4,6,7,9,9b-heptaazaphenalene-based chemicals using a theoretical approach. We have investigated the features of 1,3,4,6,7,9,9b-heptaazaphenalene and some of its trisubstituted derivatives. The substituents selected in our study contain NH_2, OH, N_3, NO_2, $-C{\equiv}N$, F, Cl, Br, $-CH{=}CH_2$, and $-C{\equiv}CH$. In this paper, we will discuss one of the substituted situations, that is, three substituents in each derivative are the same.

2. Methods

Density functional theory (DFT)[14] has been applied to optimize all of the structures and to predict harmonic vibrational frequencies. Becke's three-parameter nonlocal exchange functional along with the Lee−Yang−Parr nonlocal correlation functional (B3LYP)[15,16] is employed. Dunning's aug-cc-pVDZ (5d) basis set has been used throughout,[17] and SCF convergence criterion is set to 10^{-8}. There are no imaginary frequencies for all of the structures at this theoretical level, which suggests that all of the structures that we obtained are the structures of local minima on the potential energy surface. The natural bond orbital (NBO)[18−21] analysis has been carried out at the B3LYP/aug-cc-pVDZ level on the basis of the optimized geometries. All of these calculations were carried out using the Gaussian 98 program.[22]

---

* Corresponding authors. E-mail addresses: suqcp@mail.sc.cninfo.net (A. M. Tian); bhnbwong@cityu.edu.hk (N. B. Wong).

[†] Sichuan University.

[‡] City University of Hong Kong.

10.1021/jp035558i CCC: $27.50

The topological properties of the electronic charge density have been characterized using the atoms in molecules methodology (AIM)[23] with the AIM 2000 program package.[24]

Some of molecules discussed in the present paper may be novel candidates of high-energy density materials (HEDMs). To evaluate their HEDMs performance, we have calculated their heats of formation and relative specific impulse values introduced by Peter Politzer et al.[25] The specific impulse (I_S), widely used as a means of characterizing and evaluating explosives, is often expressed in terms of the absolute temperature in the combustion chamber T_C and the number of moles of gaseous products produced per unit weight of explosive N ($N = n/M$, where n is the number of moles of gaseous products produced by 1 mol of explosive and M is the molecular weight of explosive) by the simplified relationship given as eq 1.[26]

$$I_S \approx T_C^{1/2} N^{1/2} \tag{1}$$

This proportionality can be rationalized by kinetic theory. To apply eq 1, it is necessary to establish the identities and amounts of the various products and to determine the combustion temperature. Depending upon the composition of the explosive, the major components of the gaseous products may include CO, CO_2, N_2, H_2O, or HF with lesser quantities of other molecules and radicals such as H_2, NO, H, C, O, CHO, and N_2O.[25]

A simple approach to obtaining a rough approximation of the combustion temperature involves assuming that the heat of combustion of the explosive is used entirely to heat the product gases to the combustion temperature so that

$$-\Delta H_{\text{comb}} = C_{p,\text{gases}}(T_C - T_0) \tag{2}$$

and

$$T_C = T_0 - \frac{\Delta H_{\text{comb}}}{C_{p,\text{gases}}} \tag{3}$$

ΔH_{comb} is the enthalpy of combustion, $C_{p,\text{gases}}$ represents the total heat capacity of the gaseous products, and T_0 and T_C are the initial and the combustion temperatures. In eqs 2 and 3, it is assumed that ΔH_{comb} is constant over the temperature range between T_0 and T_C and that the pressure in the combustion chamber remains constant because of a steady-state situation; the rates of formation and discharge of product gases are taken to be equal. ΔH_{comb} can be calculated from knowledge of the molar heats of formation of the explosive and the gaseous products [eq 4].

$$\Delta H_{\text{comb}} = \sum_{i}^{\text{products}} N_i \Delta H_{\text{f},i} - N_{\text{HEDM}} \Delta H_{\text{f,HEDM}} \tag{4}$$

The molar heats of formation for gaseous products are known, while that for explosive can be determined in a number of ways; for example, a reasonable estimate can often be obtained from standard bond enthalpies plus any strain contributions. Politzer[25] has pointed out that the relative specific impulse is not highly sensitive to the method used for obtaining the heats of formation. In our work, we compute gas-phase heats of formation with the semiempirical AM1 method.

3.Results and Discussion

3.1. Properties of 1,3,4,6,7,9,9b-Heptaazaphenalene. We have investigated the geometric and electronic structure of the 1,3,4,6,7,9,9b-heptaazaphenalene composed of three s-triazines at B3LYP/aug-cc-pvDZ level. The s-triazine, a high-symmetry molecule with an aromatic heteroring, is listed for comparison.

Lancaster et al. had determined the geometrical structure of s-triazine in gas phase by Raman study.[27] Compared with their experimental results, our structural parameters show a good agreement (see Figure 1). So the computational methods that we selected in this paper are reliable. As shown in Figure 1, 1,3,4,6,7,9,9b-heptaazaphenalene has a rigid plane geometry with D_{3h} symmetry. N1−C2, C2−N3, N4−C5, C5−N6, N7−C8, and C8−N9 bond lengths are 1.334 Å, N1−C9a, N3−C3a, C3a−N4, N6−C6a, C6a−N7, and N9−C9a bond lengths are 1.337 Å, and C3a−N9b, C6a−N9b, and C9a−N9b bond lengths are 1.407 Å. We find that the periphery of this tricyclic system has a uniform bond length distribution, and they are shorter than the normal C−N single bond length (1.470 Å) and longer than the normal C═N double bond length (1.280 Å). There seems to exist a conjugation system over 1,3,4,6,7,9,9b-heptaazaphenalene. Judged from the natural bond orbital (NBO) analysis, the Wiberg bond indexes (WBIs)[19] of N1−C2, C2−N3, N4−C5, C5−N6, N7−C8, and C8−N9 are 1.40, while WBIs of N1−C9a, N3−C3a, C3a−N4, N6−C6a, C6a−N7, and N9−C9a are 1.34. These WBIs are similar to the WBIs of C−N bonds in s-triazine (1.41). The fact that all of the WBIs are between the standard values of the single bond (1.0) and the double bond (2.0) suggests that there may exist considerable conjugation over the ring. In addition, the stabilization interaction energies, $E(2)$, are calculated by means of the second-order perturbation theory. In the NBO analysis, $E(2)$ is used to describe the delocalization trend of electrons from the donor bond to the acceptor bond. The selected stabilization interaction energies $E(2)$ for the 1,3,4,6,7,9,9b-heptaazaphenalene at the B3LYP/aug-cc-pVDZ level are summarized in Table 1 and Figure 2, where BD and BD* represent bonding and antibonding natural bond orbital and LP represents lone pairs. As shown in the table and figure, there exist strong donor−acceptor interactions within this system. Interaction energies $E(2)$ between π bonding orbitals and π^* antibonding orbitals in the periphery of the system are 43.37 kcal/mol, and $E(2)$ between the lone pair of the central nitrogen atom and peripheral π^* antibonding orbitals are about 49.10 kcal/mol. These $E(2)$ are similar to the $E(2)$ between π bonding orbitals and π^* antibonding orbitals in the s-triazine molecule (38.01 kcal/mol). Moreover, molecular orbital analysis shows that there exists a delocalized π occupied orbital in the 1,3,4,6,7,9,9b-heptaazaphenalene (A) molecule. This orbital is composed purely of $2p_z$ orbitals of all carbon and nitrogen atoms, and its stereograph is drawn in Figure 3.

As discussed above, we find that the 1,3,4,6,7,9,9b-heptaazaphenalene molecule contains a large conjugation system, which means this structure is stable. We analyzed its topological properties of electron density using Bader's theory of atoms in molecules (AIM). The AIM atomic charges listed in Table 2 indicate that the formation of 1,3,4,6,7,9,9b-heptaazaphenalene results in the electron redistribution among the nitrogen and carbon atoms, compared with that in s-triazine. The net charges for all of the carbon atoms are 1.11, and those for all of the nitrogen atoms in s-triazine are −1.08. After formation of 1,3,4,6,7,9,9b-heptaazaphenalene, all of the positive charges for carbon atoms are increased, while all of the negative charges for nitrogen atoms are decreased, except that for N_{9b} has no change. More sensitive probe of the electronic structure of a molecule is provided by the Laplacian of the charge density, $\nabla_\rho^2(r)$, which determines the regions of space wherein electronic charge of a molecule is locally concentrated and depleted.[28] This function has been shown to demonstrate the existence of local

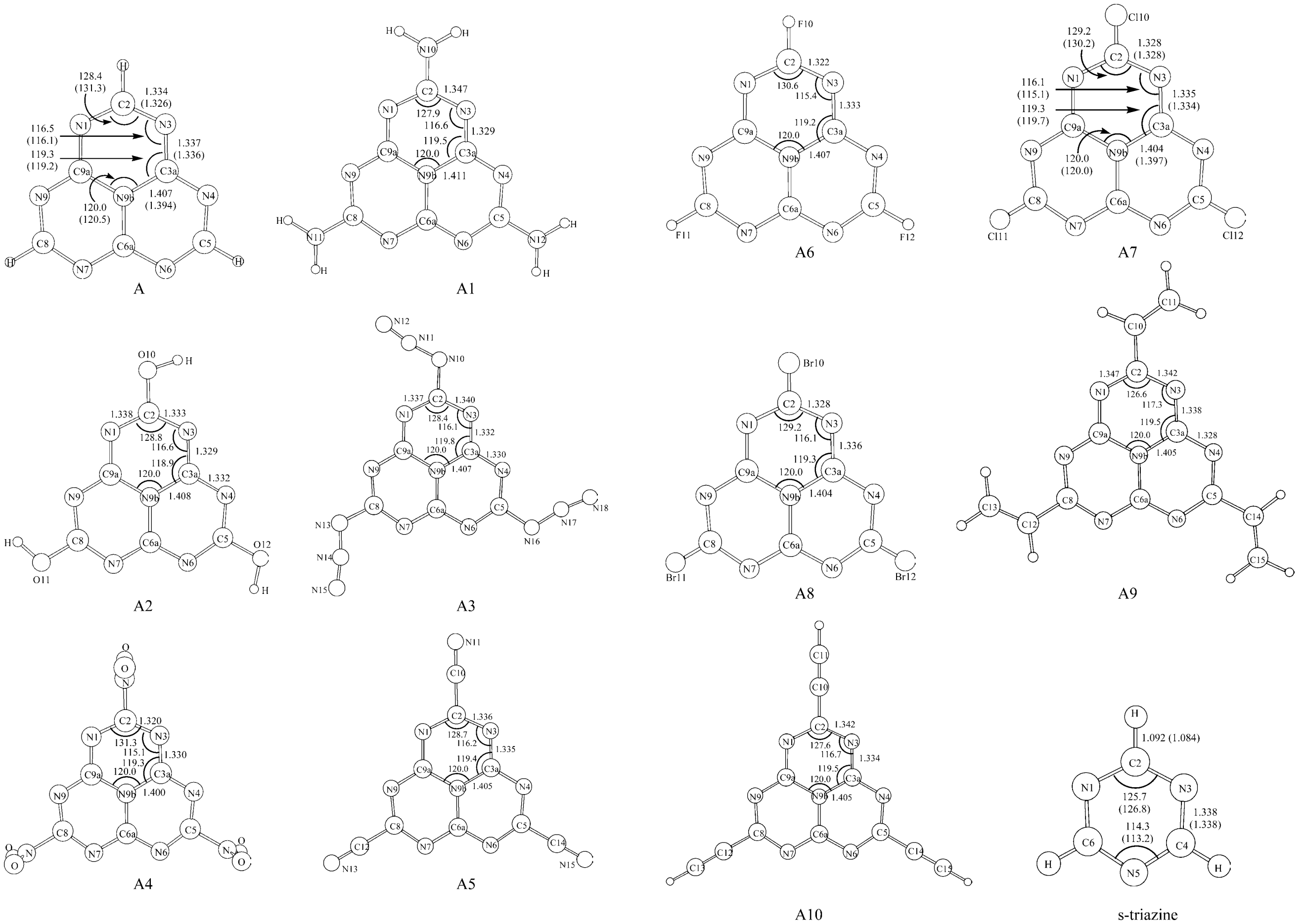

Figure 1. Optimized molecular structures for s-triazine, 1,3,4,6,7,9,9b-heptaazaphenalene (A), and its 10 derivatives (A1−A10), along with their bond lengths (in Å) and angles (in deg). Experimental data for s-triazine are listed in parentheses.

concentrations of electronic charge in both bonded and nonbonded regions of an atom in a molecule,[28,29] without recourse to any orbital model or arbitrary reference state. Interactions resulting from the sharing of charge density between atoms, as in covalent and polar bonds, are characterized by $\nabla_{\rho}^{2}(r) < 0$. The contours of the Laplacian of the charge density of s-triazine and 1,3,4,6,7,9,9b-heptaazaphenalene are drawn in Figure 4. The figure clearly indicates that $\nabla\rho^2(r)$ in 1,3,4,6,7,9,9b-heptaazaphenalene remains very similar to that in s-triazine; the electron cloud around each nitrogen atom shows a much greater concentration of charge, and a small polarization of the covalent CN bond with the lone pairs on the nitrogen atoms is clearly visible, while the nitrogen lone pairs in 1,3,4,6,7,9,9b-heptaazaphenalene are less diffuse than their counterparts in s-triazine. Here it should be emphasized that nonbonded charge concentrations are thinner in radial extent than are the bonded ones.

Vibrational analysis shows that there is a characteristic frequency (869.8 cm^{-1}) for 1,3,4,6,7,9,9b-heptaazaphenalene. Its vibrational mode is C, N out-of-plane rocking, and its infrared intensity is 35.4 km/mol. This vibrational mode has not been found in s-triazine; thus, it can be used to distinguish s-triazine and 1,3,4,6,7,9,9b-heptaazaphenalene. This difference is useful for experimental synthesis and recognition of 1,3,4,6,7,9,9b-heptaazaphenalene.

3.2. Substituent Effects on the Properties of the 1,3,4,6,7,9,9b-Heptaazaphenalene Parent Molecule. Many organic chemicals show various profound features by replacing their components such as substituents. In this section, we will discuss the substituent effects on the geometric and electronic properties of 1,3,4,6,7,9,9b-heptaazaphenalene. The substituents that we selected contain electron-donating groups, electron-withdrawing groups, and halogens, such as $-NO_2$, $-NH_2$, $-N_3$, $-OH$, $-C{\equiv}N$, $-F$, $-Cl$, $-Br$, $-CH{=}CH_2$, and $-C{\equiv}CH$. In this paper, we will just investigate a special substituted situation, that is, three substituents in each derivative are the same.

3.2.1. Effects on Geometry. We have first optimized the geometries of these trisubstituted molecules. The molecular structures, along with their geometrical parameters, are illustrated in Figure 1. It is clear that almost all of the derivatives have D_{3h} symmetry like their parent molecule A, while A_2, A_3, and A_9 degenerate to C_{3h} symmetry. The ring holds its rigid plane in all of the derivatives, and all of the substituents are in this plane except the NO_2 group. Here we must emphasize that the NH_2 group is noplanar in many molecules because of the repulsion between lone pair electrons of nitrogen and electrons of two hydrogens. But in derivative A_1, the lone pair of nitrogen interacts with the ring strongly (as seen in Table 1, $E(2)$ is 60.79 kcal/mol). So the repulsion between nitrogen and hydrogen is decreased, and this results in a planar structure.

The substituent effect on the bond lengths of C−N bonds adjacent to the substituents is relatively considerable. In the vicinity of substituents, the C−N bond lengths are 1.347 for A_1, 1.338 for A_2, 1.337 for A_3, 1.320 for A_4, 1.336 for A_5, 1.322 for A_6, 1.328 for A_7, 1.328 for A_8, 1.347 for A_9, and 1.342 Å for A_{10}. Compared with corresponding bond length 1.334 Å for parent molecule A, it is clear that when an electron-donating group such as $-NH_2$, $-N_3$, or $-OH$ is attached to the parent ring, the adjacent C−N bond lengths increase. The converse is true when an electron-withdrawing group ($-NO_2$) or a halogen ($-F$, $-Cl$, $-Br$) is attached to the parent ring. And when the

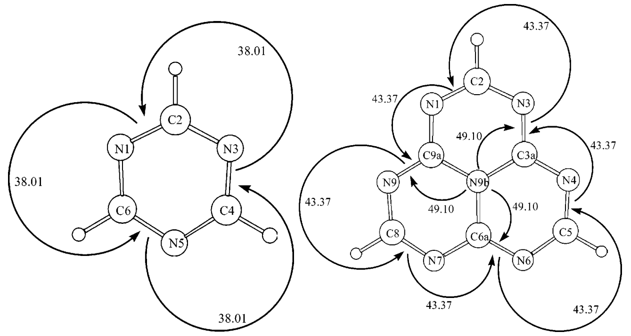

Figure 2. The stabilization interaction between π bonding orbitals and π^* antibonding orbitals and between lone pair and π^* antibonding orbitals in s-triazine and 1,3,4,6,7,9,9b-heptaazaphenalene (units of kcal/mol).

TABLE 1: Selected Stabilization Interaction Energies $E(2)$ (kcal/mol) for 1,3,4,6,7,9,9b-Heptaazaphenalene (A) and Its Ten Derivatives (A1−A10)

	donor NBO	acceptor NBO	$E(2)$
A	BD N1−C2	BD* N9−C9a	43.37
	BD N9−C9a	BD* N7−C8	43.37
	BD N7−C8	BD* N6−C6a	43.37
	BD N6−C6a	BD* N4−C5	43.37
	BD N4−C5	BD* N3−C3a	43.37
	BD N3−C3a	BD* N1−C2	43.37
	LP (1) N9b	BD* N3−C3a	49.10
	LP (1) N9b	BD* N6−C6a	49.10
	LP (1) N9b	BD* N9−C9a	49.10
A1	LP (1) N10	BD* N1−C2	60.79
	LP (1) N11	BD* N7−C8	60.79
	LP (1) N12	BD* N4−C5	60.79
A2	LP (2) O10	BD* N1−C2	45.84
	LP (2) O11	BD* N7−C8	45.84
	LP (2) O12	BD* N4−C5	45.84
A3	BD N1−C9a	BD* C2−N10	46.50
	BD C6a−N7	BD* C8−N13	46.50
	BD C3a−N4	BD* C5−N16	46.50
A5	BD C10−N11	BD* N1−C2	12.25
	BD C12−N13	BD* N7−C8	12.25
	BD C14−N15	BD* N4−C5	12.25
A6	LP (3) F10	BD* N1−C2	30.05
	LP (3) F11	BD* N7−C8	30.05
	LP (3) F12	BD* N4−C5	30.05
A7	LP (3) Cl10	BD* N1−C2	21.22
	LP (3) Cl11	BD* N7−C8	21.22
	LP (3) Cl12	BD* N4−C5	21.22
A8	LP (3) Br10	BD* N1−C2	16.72
	LP (3) Br11	BD* N7−C8	16.72
	LP (3) Br12	BD* N4−C5	16.72
A9	BD C10−C11	BD* N1−C2	19.08
	BD C12−C13	BD* N7−C8	19.08
	BD C14−C15	BD* N4−C5	19.08
A10	BD C10−C11	BD* N1−C2	17.53
	BD C12−C13	BD* N7−C8	17.53
	BD C14−C15	BD* N4−C5	17.53

substituent containing a π bond, such as $-C{\equiv}N$, $-CH{=}CH_2$, and $-C{\equiv}CH$, is attached to the parent ring, the adjacent C−N bond lengths increase.

The bond lengths of C3a−N9b, C6a−N9b, and C9a−N9b bonds connected with the central nitrogen atom are 1.407 Å for 1,3,4,6,7,9,9b-heptaazaphenalene. After substitution, these bond lengths change to 1.411 for A_1, 1.408 for A_2, 1.407 for A_3, 1.400 for A_4, 1.405 for A_5, 1.407 for A_6, 1.404 for A_7, 1.404 for A_8, 1.405 for A_9, and 1.405 Å for A_{10}. We find that when electron-donating groups, electron-withdrawing groups, and halogens are attached to the parent ring, the change trends of these three bond lengths are in agreement with that of the bonds adjacent to the substituents, whereas when the substituents containing a π bond are attached to the parent ring, these three bond lengths decrease, which is the reverse of the change trends of those bonds adjacent to the substituents.

TABLE 2: The AIM Atomic Charges for s-Triazine and 1,3,4,6,7,9,9b-Heptaazaphenalene[a]

s-triazine		1,3,4,6,7,9,9b-heptaazaphenalene	
atom	charge	atom	charge
N1	−1.08	N1	−0.97
C2	1.11	C2	1.18
N3	−1.08	N3	−0.99
C4	1.11	C3a	1.43
N5	−1.08	N4	−0.99
C6	1.11	C5	1.18
		N6	−0.99
		C6a	1.43
		N7	−0.98
		C8	1.18
		N9	−0.97
		C9a	1.43
		N9b	−1.08

[a] The integration radius is 0.5 au for all the atoms.

3.2.2. Effects on Electronic Structures. These geometric variations are consistent with the topological properties of electron density at the bond critical points. The Laplacian of electron density, $\nabla_\rho^2(r)$, at the bond critical points of the C−N bond adjacent to the substituents is, respectively, −1.154 for A_1, −1.206 for A_2, −1.179 for A_3, −1.294 for A_4, −1.218 for A_5, −1.312 for A_6, −1.252 for A_7, −1.255 for A_8, −1.167 for A_9, and −1.187 for A_{10}. Compared with the corresponding $\nabla_\rho^2(r)$ of −1.232 for parent molecule A, it is worth stressing that the introduction of electron-withdrawing groups ($-NO_2$) or halogens (−F, −Cl, −Br) makes $\nabla_\rho^2(r)$ more negative, which means that the corresponding C−N bond is strengthened. Conversely, $\nabla_\rho^2(r)$ is less negative when the electron-donating groups, $-NH_2$, $-N_3$, or −OH, or those substituents containing a π bond, $-C{\equiv}N$, $-CH{=}CH_2$, and $-C{\equiv}CH$, are attached, which means the corresponding C−N bond is weakened.

Electron distribution of a molecule also could be described by the molecular electrostatic potential (MEP).[30−32] The electrostatic potential at a spatial point r around a molecule is (in atomic units)[33]

$$V(r) = \sum_{A} \frac{Z_A}{|R_A - r|} - \int \frac{\rho(r')}{|r - r'|} \, dr'$$

where Z_A is the charge on nucleus A located at R_A. The first term on the right-hand side of the equation represents the effect of the nuclei and the second is that of the electron density. $V(r)$ is then the net electrostatic effect resultant from the total molecular charge distribution (nuclei plus electrons). The sign of $V(r)$ indicates thus the regions where either nuclei or electrons dominate, so an approaching electrophile will be drawn to points where $V(r) < 0$, particularly the local minima. The MEP is an important analytical tool in the study of molecular reactivity and particularly useful when visualized on surfaces or in regions of space because it provides information about local polarity. Typically, after having chosen some sort of region to be visualized, one chooses a color-coding convention to depict the MEP.[34] In this paper, the most negative potential is assigned to be blue, the most positive potential is assigned to be red, and the color spectrum is mapped to all other values by linear interpolation. Figure 5 summarizes the shape and position of MEP observed. The electrostatic behavior of these molecules as given by MEP shows a clear and marked separation between the negative spatial domains and the positive domain that covers

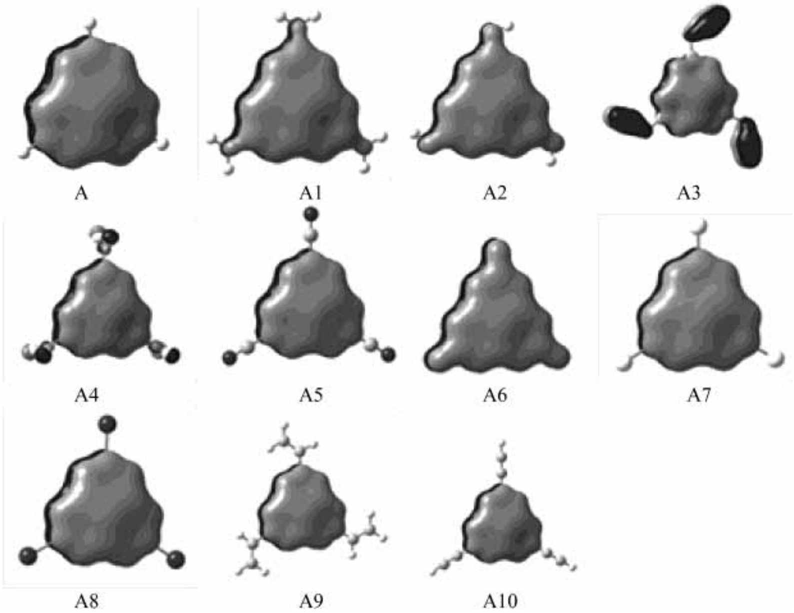

Figure 3. The delocalized π occupied orbitals in 1,3,4,6,7,9,9b-heptaazaphenalene (A) and its 10 derivatives (A1−A10).

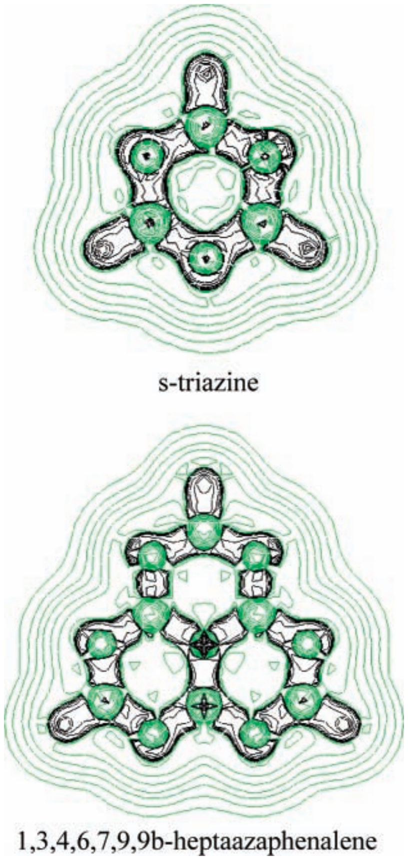

Figure 4. The contour map of $\nabla_{\rho}^2(r)$ in the molecular plane for s-triazine and 1,3,4,6,7,9,9b-heptaazaphenalene. Positive values of $\nabla_{\rho}^2(r)$ are denoted by green contours and negative values by black contours.

the whole space surrounding the ring. When an electron-donating group such as $-NH_2$, $-N_3$, or $-OH$ is attached to the parent ring, the negative spatial domains are extended mildly. The same result could be obtained by the attachment of substituent containing a π bond such as $-CH{=}CH_2$ or $-C{\equiv}CH$ to the parent ring. However, if the substituent is an electron-withdrawing group ($-NO_2$) or a halogen ($-F$, $-Cl$, $-Br$), the negative spatial domains will shrink, split, and even vanish. A special substituent is $-C{\equiv}N$; when this group is attached to the ring, the old negative spatial domains of the ring vanish and new negative spatial domains emerge near the cyanophoric nitrogen.

The net charge distribution in the studied compounds was analyzed by means of the natural bond orbital (NBO) analysis. In Table 3, we have listed some selected natural atomic charges. The results indicate that the substitution of all of the substituents increases the magnitudes of positive charges on connective carbons C_2, C_5, and C_8. The negative charges of central nitrogen N_{9b} are increased in all of the derivatives except in A_4 and A_5. To other nitrogen atoms of the ring, their negative charges are increased in A_1, A_2, A_3, A_6, and A_9, while decreased in A_4, A_5, A_7, A_8, and A_{10}.

The second-order perturbation stabilization energies $E(2)$ obtained by NBO analysis are summarized in Table 1. It can be used to describe the interaction between the substituents and the parent ring. In NBO analysis, if the stabilization interaction energy $E(2)$ between a donor bonding orbital and an acceptor bonding orbital is large, there is strong interaction between the two bonds. In Table 1, only the stabilization energies between donor π orbital and acceptor π^* orbital or donor lone pair orbital and acceptor π^* orbital are listed. The $E(2)$ values smaller than 10 kcal/mol are not included in Table 1, as these interactions may be deemed as weak. According to the table, there is strong donor−acceptor interactions between the lone pair orbitals on nitrogen, oxygen, and halogen atoms in $-NH_2$, $-N_3$, $-OH$, $-F$, $-Cl$, and $-Br$ groups and the π^* orbitals in the ring. And donor−acceptor interactions also exist between the π orbitals of $-C{\equiv}N$, $-CH{=}CH_2$, and $-C{\equiv}CH$ groups and the π^* orbitals in the ring. Only for A_4, there is no strong interaction between $-NO_2$ and the ring; this is caused by two reasons. First, there is no lone pair on the N_{NO_2} atom to provide a lone pair orbital as a donor. Second, the N−O π orbital of $-NO_2$ group is composed of $2p_x$ orbitals of nitrogen and oxygen atoms, while the N−C π orbital of the ring is composed of $2p_z$ orbitals of nitrogen and carbon atoms; the orientations of these two π orbitals are perpendicular and thus hinders the interaction between these two orbitals. As a result of interaction between substituents and the ring, the natural bond orbital energies of the N−C bond adjacent to the substituents are decreased from −0.8816 for A to −0.8868 for A_2, −0.8933 for A_3, −0.9672

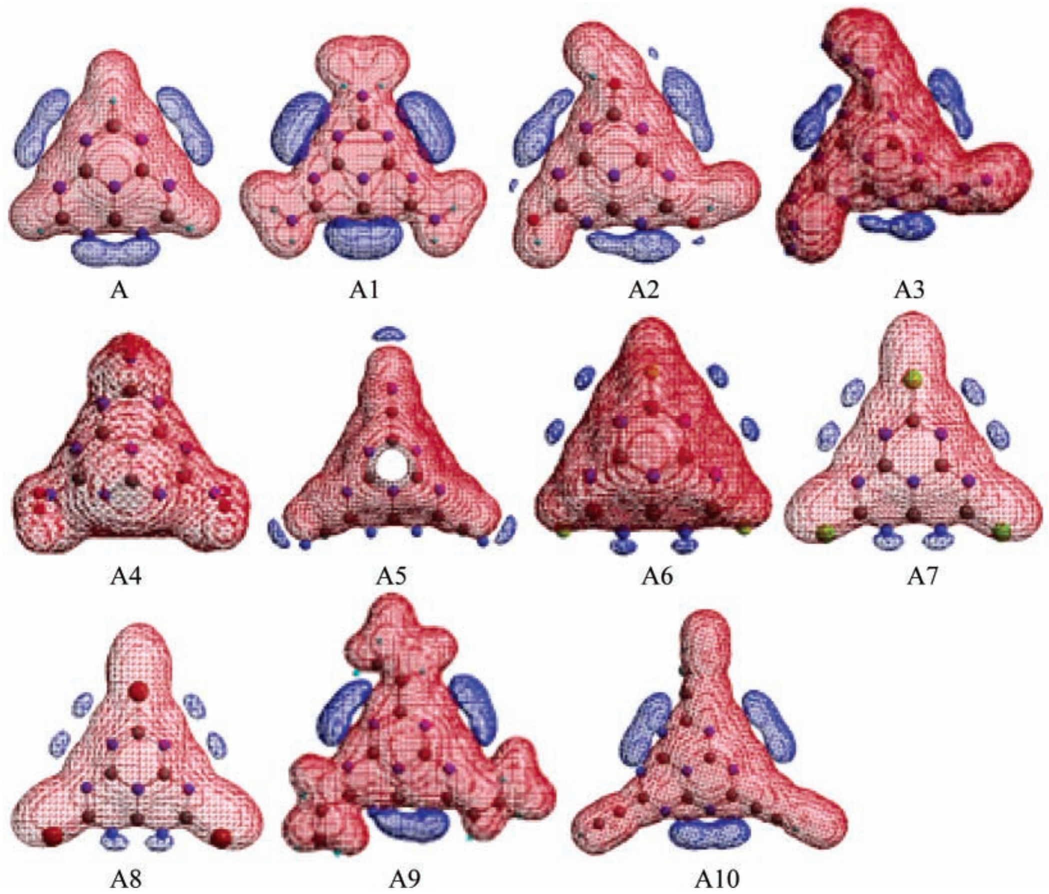

Figure 5. The MEP surfaces for the 1,3,4,6,7,9,9b-heptaazaphenalene (A) and its 10 derivatives (A1−A10). The most negative potential is assigned to be blue, the most positive potential is assigned to be red, and the color spectrum is mapped to all other values by linear interpolation.

TABLE 3: Selected Natural Atomic Charges for 1,3,4,6,7,9,9b-Heptaazaphenalene (A) and Its Ten Derivatives (A1−A10)

	A	A1	A2	A3	A4	A5	A6	A7	A8	A9	A10
N1	−0.55	−0.61	−0.62	−0.55	−0.52	−0.49	−0.57	−0.54	−0.54	−0.55	−0.52
C2	0.36	0.66	0.81	0.64	0.65	0.41	0.91	0.46	0.39	0.47	0.44
N3	−0.55	−0.61	−0.58	−0.59	−0.51	−0.49	−0.57	−0.54	−0.54	−0.56	−0.52
C3a	0.68	0.69	0.69	0.69	0.70	0.69	0.69	0.69	0.69	0.69	0.69
N4	−0.55	−0.61	−0.62	−0.55	−0.51	−0.49	−0.57	−0.54	−0.54	−0.55	−0.52
C5	0.36	0.66	0.81	0.64	0.63	0.41	0.91	0.46	0.39	0.47	0.44
N6	−0.55	−0.61	−0.58	−0.59	−0.51	−0.49	−0.57	−0.54	−0.54	−0.56	−0.52
C6a	0.68	0.69	0.69	0.69	0.70	0.69	0.69	0.69	0.69	0.69	0.69
N7	−0.55	−0.61	−0.62	−0.55	−0.51	−0.49	−0.57	−0.54	−0.54	−0.55	−0.52
C8	0.36	0.66	0.81	0.64	0.64	0.41	0.91	0.46	0.39	0.47	0.44
N9	−0.55	−0.61	−0.58	−0.59	−0.51	−0.49	−0.57	−0.54	−0.54	−0.56	−0.52
C9a	0.68	0.69	0.69	0.69	0.70	0.69	0.69	0.69	0.69	0.69	0.69
N9b	−0.47	−0.51	−0.50	−0.49	−0.46	−0.46	−0.48	−0.47	−0.47	−0.48	−0.47

for A_4, −0.9341 for A_5, −0.9287 for A_6, −0.9288 for A_7, and −0.9295 au for A_8 but increased to −0.8418 for A_1, −0.8600 for A_9 and −0.8766 au for A_{10}.

3.2.3. Effect on Conjugation of the Parent Ring. From Figure 1, it can be seen that the bond lengths of the periphery of the ring for all of the derivatives range from 1.310 to 1.347 Å and just locate between the normal C−N single bond length (1.470 Å) and the normal C=N double bond length (1.280 Å). Judged from the bond lengths, it seems that the conjugation system over the ring still exists in the derivatives. Moreover, judged from the NBO analysis, the Wiberg bond indexes (WBIs) of all of the peripheral bonds of the ring are in the range of 1.28−1.40. The fact that these values lie between the standard values of the single bond (1.0) and the double bond (2.0) suggests that there may exist considerable conjugation over the ring. In addition, NBO results show that there exist strong donor−acceptor interactions between π bonding orbitals and π^* antibonding orbitals in the periphery of the ring ($E(2)$ is about 40 kcal/mol) and between lone pair of central nitrogen atom and peripheral π^* antibonding orbitals ($E(2)$ is about 45 kcal/mol). Through molecular orbital analysis, we find a delocalized π occupied orbital that id composed purely of $2p_z$ orbitals of all carbon and nitrogen atoms of the ring in all derivatives. Here we must emphasize that the central nitrogen atom N9b participates in the conjugation, which is an advantage to the stability of the ring. As discussed above, the large conjugation system still exists in all derivatives.

3.2.4. Effect on HOMO and LUMO. The analysis of the molecular orbitals can provide much useful information about a molecule, such as the site of electron attachment and detachment, as well as chemical reactivity,[35] and HOMO−LUMO gaps in close agreement with λ_{max} values from UV spectroscopy.[36] Moreover, in HF calculation, it is possible to obtain ionizational potential (IP) and electron affinity (EA) from

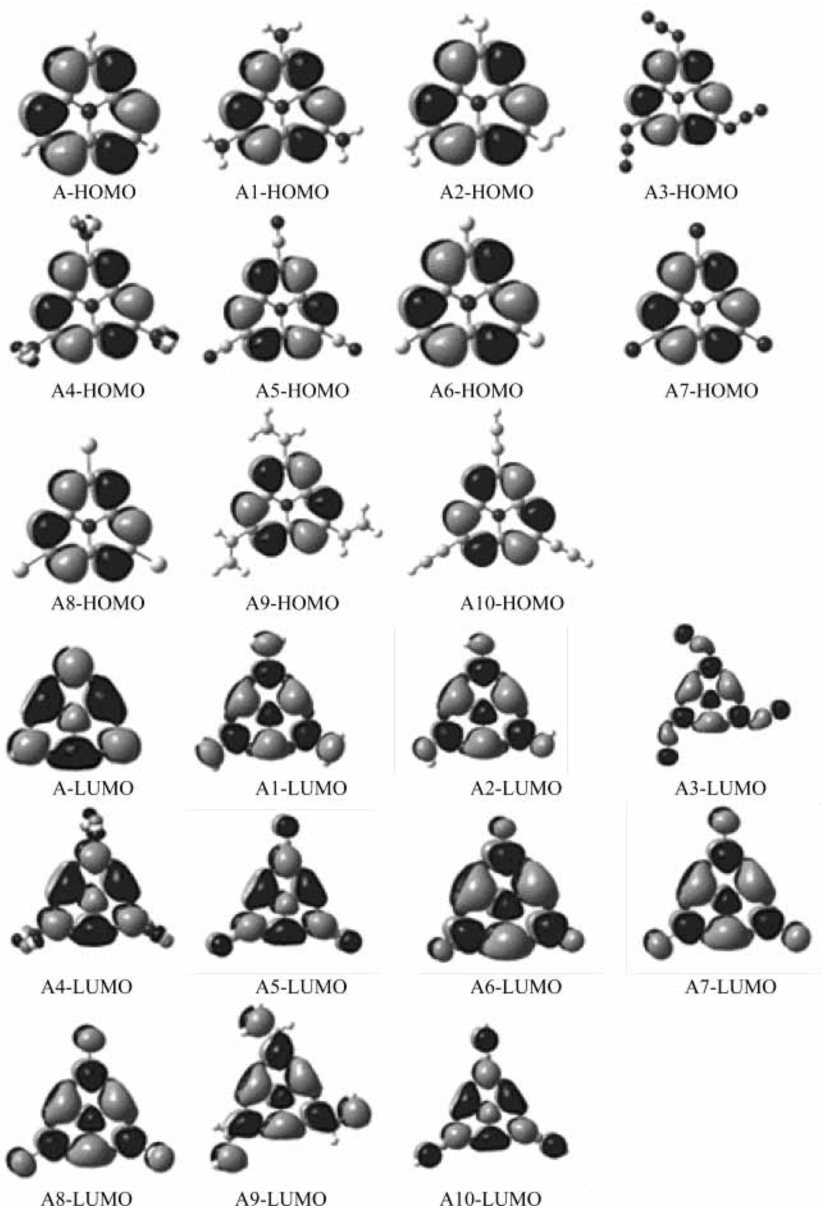

Figure 6. The HOMO and LUMO molecular orbitals for 1,3,4,6,7,9,9b-heptaazaphenalene (A) and its 10 derivatives (A1−A10).

the corresponding HOMO and LUMO eigenvalues according to Koopmans theorem.[37]

The shape and location of the frontier orbitals, that is, HOMO and LUMO, of all molecules are illustrated in Figure 6. It is observed that all of the substituents interact mainly with the LUMO orbital, whereas their interaction with the HOMO is minor. The HOMO of each molecule is only localized on the peripheral nitrogen atoms of the ring and has π^* antibonding character. It is a component of the $2p_z$ orbitals of these nitrogen atoms. The LUMO is shared by all of the atoms in a molecule and made up of $2p_z$ orbitals of these atoms.

The calculated results for the HOMO and LUMO energies are listed in Table 4. It shows a comparison of the energetics of different substituted molecules. It is clear from this table that when $-NH_2$, $-CH{=}CH_2$, or $-C{\equiv}CH$ group is attached to the ring, the HOMO energy level increases, whereas the attachment of other group such as $-OH$, $-N_3$, $-NO_2$, $-C{\equiv}N$, $-F$, $-Cl$, or $-Br$ will make HOMO energy level decreased. As for LUMO energy level, when $-NH_2$, $-OH$, $-N_3$, or $-CH{=}CH_2$ group is attached to the ring, it will increase and the converse is true when other groups like $-NO_2$, $-F$, $-Cl$, $-Br$, $-C{\equiv}CH$, or $-C{\equiv}N$ is attached to the ring.

TABLE 4: The HOMO and LUMO Energies and the Energy Gap for 1,3,4,6,7,9,9b-Heptaazaphenalene (A) and Its Ten Derivatives (A1−A10)

molecule	E_{HOMO} (eV)	E_{LUMO} (eV)	$\Delta E_{LUMO-HOMO}$ (eV)
A	−7.32	−3.40	3.92
A1	−6.44	−1.52	4.92
A2	−7.34	−2.58	4.76
A3	−7.48	−3.34	4.14
A4	−8.91	−4.85	4.06
A5	−8.61	−5.08	3.53
A6	−8.14	−3.64	4.50
A7	−7.92	−3.76	4.16
A8	−7.88	−3.76	4.12
A9	−6.84	−3.19	3.65
A10	−7.28	−3.69	3.59

However, the effects of all electron-withdrawing groups, electron-donating groups, and halogens are found to be similar with respect to the HLG (HOMO−LUMO gap); that is, in both cases, the derivatives increase the HLG as compared to the

TABLE 5: Selected Harmonic Vibrational Frequencies and Infrared (IR) Intensities of 1,3,4,6,7,9,9b-Heptaazaphenalene and Its Ten Derivatives

molecule	frequency (cm^{-1})	IR intensity (km/mol)	vibrational mode	exptl value (cm^{-1})
2,4,6-triamino-s-triazine	828.0	34.9	ring out-of-plane rocking	813
	3615.6	120.8	amino asymmetry stretch	3500
2,4,6-trifluoro-s-triazine,	828.4	41.6	ring out-of-plane rocking	806
	1087.3	129.3	C−F stretching	1070
2,4,6-trihydroxyl-s-triazine	835.7	56.9	ring out-of-plane rocking	807
	3759.1	157.1	hydroxy asymmetry stretch	3500
A	869.8	35.4	ring out-of-plane rocking	
	3179.4	20.3	C−H asymmetry stretch	
A1	833.9	55.1	ring out-of-plane rocking	
	3748.4	99.2	amino asymmetry stretch	
A2	844.5	64.5	ring out-of-plane rocking	
	3750.7	212.7	hydroxy asymmetry stretch	
A3	843.0	43.8	ring out-of-plane rocking	
	2281.2	922.4	azide group N−N asymmetry stretch	
A4	858.3	27.8	ring out-of-plane rocking	
	1657.4	896.441	nitryl N−O symmetry stretching	
A5	860.8	36.8	ring out-of-plane rocking	
	2353.3	87.1	cyano C−N asymmetric stretch	
A6	851.8	47.383	ring out-of-plane rocking	
	1435.7	1124.7	C−F stretching	
A7	850.4	31.2	ring out-of-plane rocking	
	1324.3	906.0	C−Cl stretching	
A8	848.3	28.1	ring out-of-plane rocking	
	1308.1	970.9	C−Br stretching	
A9	868.3	52.8	ring out-of-plane rocking	
	1691.1	59.9	ethenyl C−C asymmetric stretch	
A10	857.9	42.2	ring out-of-plane rocking	
	2227.1	204.7	ethynyl C−C asymmetric stretch	

parent molecule, reflecting a shift toward higher frequencies in their electronic absorption spectra. But when a group containing a π bond, such as $-CH{=}CH_2$, $-C{\equiv}CH$, or $-C{\equiv}N$, is substituted in the parent ring, the HLG is reduced, reflecting a shift toward lower frequencies in their electronic absorption spectra.

3.2.5. Effect on Vibrational Frequency. To support future experimental verification of 1,3,4,6,7,9,9b-heptaazaphenalene and its derivatives structures, the harmonic vibrational frequencies of these compounds are computed at the B3LYP/aug-cc-pVDZ level.

Some selected harmonic vibrational frequencies and infrared (IR) intensities of 1,3,4,6,7,9,9b-heptaazaphenalene and its 10 derivatives are presented in Table 5. To check the accuracy of our calculated values and to demonstrated the trends in vibrational modes for the related molecules, we also provide in Table 5 the vibrational frequencies and corresponding infrared intensities of 2,4,6-triamino-s-triazine, 2,4,6-trifluoro-s-triazine, and 2,4,6-trihydroxyl-s-triazine, computed at the same level of theory along with the experimental (in parentheses) values[38] available in the literature. According to the table, we find that the characteristic frequency of the parent ring is around 830−870 cm^{-1} and its vibrational mode is C, N out-of-plane rocking. This characteristic frequency is very close to that of the s-triazine ring (about 820 cm^{-1}), and the substitution of all of the substituents makes it shift to a lower wavenumber. The infrared intensity of this characteristic frequency ranges from 28 to 64 km/mol in the derivatives. Comparably, the infrared intensity of the substituent is strong. The intensities of amino N−H symmetric stretch (3604 cm^{-1}), hydroxy O−H asymmetric stretch (3750 cm^{-1}), azide N−N asymmetric stretch (2281 cm^{-1}), nitro N−O symmetric stretch (1657 cm^{-1}), C−F asymmetric stretch (1436 cm^{-1}), C−Cl asymmetric stretch (1324 cm^{-1}), C−Br asymmetric stretch (1308 cm^{-1}), ethynyl C−C asymmetric stretch (2227 cm^{-1}), ethenyl C−C asymmetric stretch (1691 cm^{-1}), and cyano C−N asymmetric stretch (2353 cm^{-1}) are, respectively, 227, 213, 922, 896, 1125, 908, 970, 204, 60, and 85 km/mol.

3.3 Potential Candidates for High-Energy Density Materials. Nitrogen-rich compounds have attracted interest as well on account of their possible use as high-energy density materials (HEDMs).[39−42] Bartlett[39] suggested some nitrogen-rich clusters formed by N, O, and H as HEDMs. Hammerl and Klapötke studied nitrogen-rich clusters CN_x in both experiment and theory.[40] The nitrogen-rich compounds form a unique class of energetic materials deriving most of their very high positive heats of formation rather than from oxidation of the carbon backbone, as with traditional energetic materials.[43,44] Usually, high heats of formation would decrease the stability of a compound. So the difficulty in identifying nitrogen-rich HEDMs candidates lies in finding molecules that not only have high heats of formation but also could exist stably. All of the compounds discussed in this paper have a big conjugated system, which would increase the molecular stability. If their heats of formation are high enough, maybe they can form a class of novel nitrogen-rich HEDMs.

The heat of formation, which is frequently taken to be indicative of the “energy content” of a HEDM, is calculated for 1,3,4,6,7,9,9b-heptaazaphenalene and its derivatives. Moreover, as mentioned earlier, the specific impulse is also calculated to evaluate the performance of all of these compounds as HEDMs. To facilitate comparisons, our values are given relative to HMX (1,3,5,7-tetranitro-1,3,5,7-tetraazacyclooctane), a widely used HEDM. In Table 6 are given idealized stoichiometric decomposition reactions for HMX, 1,3,4,6,7,9,9b-heptaazaphenalene, and its 10 derivatives. According to Politzer et al,[25] all nitrogens are assumed to go to N_2, carbons to C or CO (if oxygens are available), and fluorines, chlorines, and bromines to F_2, Cl_2, and Br_2, while oxygens preferentially form H_2O (if hydrogens are available) and otherwise CO and CO_2 in that order. We use such reactions to calculate the quantity n/M in which n is the number of moles of gaseous products and M is

TABLE 6: Idealized Stoichiometric Decomposition Reactions and Some Properties of HMX, 1,3,4,6,7,9,9b-Heptaazaphenalene, and Its Ten Derivatives

molecule	reaction	n/M	$(n/M)^{1/2}$	relative $\Delta_f H$	relative I_s
HMX	$C_4N_8O_8H_8 \rightarrow 4CO + 4N_2 + 4H_2O$	0.0405	0.2013	1	1
A	$C_6N_7H_3 \rightarrow {}^{7}/_{2}N_2 + {}^{3}/_{2}H_2 + 6C$	0.0289	0.1700	1.34	0.73
A1	$C_6N_{10}H_6 \rightarrow 5N_2 + 6C + 3H_2$	0.0367	0.1916	1.42	0.72
A2	$C_6N_7O_3H_3 \rightarrow {}^{7}/_{2}N_2 + {}^{3}/_{2}CO + {}^{3}/_{2}H_2O + {}^{9}/_{2}C$	0.0294	0.1715	0.59	0.71
A3	$C_6N_{16} \rightarrow 8N_2 + 6C$	0.0270	0.1644	3.42	0.93
A4	$C_6N_{10}O_6 \rightarrow 5N_2 + 6CO$	0.0357	0.1890	2.00	0.97
A5	$C_9N_{10} \rightarrow 5N_2 + 9C$	0.0202	0.1420	2.31	0.75
A6	$C_6N_7F_3 \rightarrow {}^{7}/_{2}N_2 + {}^{3}/_{2}F_2 + 6C$	0.0220	0.1484	0.76	0.49
A7	$C_6N_7Cl_3 \rightarrow {}^{7}/_{2}N_2 + {}^{3}/_{2}Cl_2 + 6C$	0.0180	0.1341	1.34	0.57
A8	$C_6N_7Br_3 \rightarrow {}^{7}/_{2}N_2 + {}^{3}/_{2}Br_2 + 6C$	0.0122	0.1104	1.55	0.49
A9	$C_{12}N_7H_9 \rightarrow {}^{7}/_{2}N_2 + {}^{9}/_{2}H_2 + 12C$	0.0319	0.1785	1.77	0.69
A10	$C_{12}N_7H_3 \rightarrow {}^{7}/_{2}N_2 + {}^{3}/_{2}H_2 + 12C$	0.0204	0.1429	2.70	0.77

the molecular weight of the compounds. n/M provides a rough (and quickly determined) estimate of the number of moles of gaseous products available per unit weight of compound. Also included in Table 6 are relative heats of formation obtained from calculated values in units of calories per gram.

Our calculated results point out quite clearly that A_3 with the azide group and A_4 with the nitro group are potential candidates for HEDMs. Their relative specific impulses (I_s, compared with HMX) are 0.93 for A_3 and 0.97 for A_4. The introduction of azide and nitro groups increases specific impulses, and this can be attributed to the greater heats of formation of these compounds. The relative heats of formation are 3.42 for A_3 and 2.00 for A_4.

4. Summary

In this study, we have investigated the geometries, electronic structures, substituent effects, harmonic vibrational frequencies, and high-energy density material properties of 1,3,4,6,7,9,9b-heptaazaphenalene and its 10 derivatives. 1,3,4,6,7,9,9b-Heptaazaphenalene has a rigid plane geometry with D_{3h} symmetry, and considerable conjugation exists over the heterocycle, which is an advantage to its stability. From vibrational analysis, the ring has a characteristic frequency at 869.8 cm^{-1}, which could be used to distinguish 1,3,4,6,7,9,9b-heptaazaphenalene from s-triazine. The electronic distribution in 1,3,4,6,7,9,9b-heptaazaphenalene is very similar to that in s-triazine. When an electron-donating group or a substituent containing a π bond is attached to the parent ring, the bond lengths of C−N bonds adjacent to the substituents increase, while when an electron-withdrawing group or a halogen is attached, these bond lengths decrease. However, in all these cases, the parent ring always holds its rigid plane. MEP study shows that introduction of electron-donating groups and substituents contain π bond except $-C\equiv N$ to the parent ring will extend the negative spatial domains mildly, whereas introduction of electron-withdrawing groups or halogens will shrink, split, and even vanish the negative spatial domains. A special case is that when the $-C\equiv N$ group is attached to the ring, the negative spatial domains emerge near the cyanophoric nitrogen. To all substituent compounds, calculation results indicate that the large conjugation system still exists, and the characteristic frequency of parent ring is around 830−870 cm^{-1}, which shifts to a lower wavenumber compared with that in 1,3,4,6,7,9,9b-heptaazaphenalene. Molecular orbital study shows that the LUMO of all of the derivatives is shared by all of the atoms, while the HOMO is only localized on the peripheral nitrogen atoms of the ring. All of the HOMO and LUMO are components of $2p_z$ atomic orbitals. The introduction of a group containing a π bond to the parent ring will result in the decrease of HOMO and LUMO energy gap. Moreover, our study shows that some of our discussed compounds may be potential candidates for high-energy density materials (HEDMs).

Acknowledgment. This work was supported by the Research Grants Council of Hong Kong (Project No. 9040742 CityU 1114/02P), Special Research Foundation of Doctoral Education of Chinese University (Grant 20020610024), and the National Science Foundation of China (Grant 298730029).

Supporting Information Available: The process of calculation of relative specific impulse. This material is available free of charge via the Internet at http://pubs.acs.org.

References and Notes

(1) Fulscher, M. P.; Andersson, K.; Roos, B. O. *J. Phys. Chem.* **1992**, *96*, 9204.

(2) Innes, K. K.; Roos, I. G.; Moomaw, W. R. *J. Mol. Spectrosc.* **1988**, *132*, 492.

(3) Zhan, Z.; Müllner, M.; Lercher, J. A. *Catal. Today* **1996**, *27*, 167.

(4) Korkin, A. A.; Bartlett, R. J. *J. Am. Chem. Soc.* **1996**, *118*, 12244.

(5) Wilson, E. K. *Chem. Eng. News* **2000**, *78* (32), 62.

(6) Liebig, J. *Ann. Pharm.* **1834**, *10*, 10.

(7) Gmelin, L. *Ann. Pharm.* **1835**, *15*, 252.

(8) Pauling, L.; Sturdivant, J. H. *Proc. Natl. Acad. Sci. U.S.A.* **1937**, *23*, 615.

(9) Rossman, M. A.; Leonard, N. J.; Urano, S.; LeBreton, P. R. *J. Am. Chem. Soc.* **1985**, *107*, 3884.

(10) Hosmane, R. S.; Rossman, M. A.; Leonard, N. J. *J. Am. Chem. Soc.* **1982**, *104*, 5497.

(11) Shahbaz, M.; Urano, S.; LeBreton, P. R.; Rossman, M. A.; Hosmane, R. S.; Leonard, N. J. *J. Am. Chem. Soc.* **1984**, *106*, 2805.

(12) Rossman, M. A.; Hosmane, R. S.; Leonard, N. J. *J. Phys. Chem.* **1984**, *88*, 4324.

(13) Kroke, E.; Schwarz, M.; Bordon, E. H.; Kroll, P.; Noll, B.; Norman, A. D. *New J. Chem.* **2002**, *26*, 508.

(14) Parr, R. G.; Yang, W. *Density-functional Theory of Atoms and Molecules*; Oxford University Press: New York, 1989.

(15) Becke, A. D. *J. Chem. Phys.* **1993**, *98*, 5648.

(16) Lee, C.; Yang, W.; Parr, R. G. *Phys. Rev. B* **1988**, *37*, 785.

(17) Woon, D. E.; Dunning, T. H. *J. Chem. Phys.* **1993**, *98*, 1358.

(18) Carpenter, J. E.; Weinhold, F. *J. Mol. Struct. (THEOCHEM)* **1988**, *169*, 41.

(19) Reed, A. E.; Curtiss, L. A.; Weinhold, F. *Chem. Rev.* **1988**, *88*, 899.

(20) Foster, J. P.; Weinhold, F. *J. Am. Chem. Soc.* **1980**, *102*, 7211.

(21) Reed, A. E.; Weinstock, R. B.; Weinhold, F. J. *Chem. Phys.* **1985**, *83*, 735.

(22) Frisch, M. J.; Trucks, G. W.; Schlegel, H. B.; Scuseria, G. E.; Robb, M. A.; Cheeseman, J. R.; Zakrzewski, V. G.; Montgomery, J. A., Jr.; Stratmann, R. E.; Burant, J. C.; Dapprich, S.; Millam, J. M.; Daniels, A. D.; Kudin, K. N.; Strain, M. C.; Farkas, O.; Tomasi, J.; Barone, V.; Cossi, M.; Cammi, R.; Mennucci, B.; Pomelli, C.; Adamo, C.; Clifford, S.; Ochterski, J.; Petersson, G. A.; Ayala, P. Y.; Cui, Q.; Morokuma, K.; Malick, D. K.; Rabuck, A. D.; Raghavachari, K.; Foresman, J. B.; Cioslowski, J.; Ortiz, J. V.; Stefanov, B. B.; Liu, G.; Liashenko, A.; Piskorz, P.; Komaromi, I.; Gomperts, R.; Martin, R. L.; Fox, D. J.; Keith, T.; Al-Laham, M. A.; Peng, C. Y.; Nanayakkara, A.; Gonzalez, C.; Challacombe, M.; Gill, P. M. W.; Johnson, B. G.; Chen, W.; Wong, M. W.; Andres, J. L.; Head-Gordon,

M.; Replogle, E. S.; Pople, J. A. *Gaussian 98*, revision A.11; Gaussian, Inc.: Pittsburgh, PA, 1998.

(23) Bader, R. F. W. *Atoms in Molecules, A Quantum Theory*; International Series of Monographs in Chemistry; Oxford University Press: Oxford, U.K., 1990; Vol. 22.

(24) Biegler-König, F.; Schönbohm, J.; Derdau, R.; Bayles, D.; Bader, R. F. W. *AIM 2000*, version 2.0; McMaster University: 2002.

(25) Politzer, P.; Murray, J. S.; Grice, M. E.; Sjoberg, P. In *Chemistry of Energetic Materials*; Olah, G. A., Squire, D. R., Eds.; Academic Press: San Diego, CA, 1991; pp 77−93.

(26) Mayer, R. *Explosives*; VCH: Weinheim, W. Germany, 1987.

(27) Lancaster, J. E.; Stoicheff, B. P. *Can. J. Phys.* **1956**, *34*, 1016.

(28) Bader, R. F. W.; Essen, H. *J. Chem. Phys.* **1984**, *80*, 1943.

(29) Bader, R. F. W.; MacDougall, P. J.; Lau, C. D. H. *J. Am. Chem. Soc.* **1984**, *106*, 1594.

(30) Politzer, P.; Murray, J. S. In *Molecular Electrostatic Potentials: Concepts and Applications*; Murray, J. S., Sen, K. D., Eds.; Elsevier: Amsterdam, 1996; p 649.

(31) Boris, B.; Petia, B. *J. Phys. Chem. A* **1999**, *103*, 6793.

(32) Gadre, S. R.; Bhadane, P. K. *J. Phys. Chem. A* **1999**, *103*, 3512.

(33) Murray, J. S.; Politzer, P. In *Encyclopedia of Computational Chemistry*; Schleyer, P. R.; Wiley: New York, 1998; Vol. 2, p 912.

(34) Cramer, C. J. *Essential of Computational Chemistry: Theories and Models*; Willy: Baffins Lane, England, 2002; p 278.

(35) Fukui, K. *Theory of Orientation and Stereoselection, Reactivity and Structure, Concepts in Organic Chemistry*, Springer: Berlin, 1975; Vol. 2.

(36) Salzner, U. *Synth. Met.* **1999**, 101, 482.

(37) Szabo, A.; Ostlund, N. S. *Modern Quantum Chemistry: Introduction to Advanced Electronic Structure Theory*; McGrawHill: New York, 1982.

(38) Pouchert, C. J. *The Aldrich Library of Infrared Spectra*; Aldrich Chemical Co.: Milwaukee, WI, 1981.

(39) Bartlett, R. *Chem. Ind.* **2000**, *21*, 140.

(40) Hammerl, A.; Klapötke, T. M. *Inorg. Chem.* **2002**, *41*, 906.

(41) Gagliardi, L.; Pyykkö, P. J. *J. Am. Chem. Soc.* **2001**, *123*, 9700.

(42) Gagliardi, L.; Pyykkö, P. J. *J. Phys. Chem. A* **2002**, *106*, 4690.

(43) Zhang, M. X.; Eaton, P. E.; Gilardi, R. D. *Angew. Chem.* **2000**, *112*, 422.

(44) Zhang, M. X.; Eaton, P. E.; Gilardi, R. D. *Angew. Chem., Int. Ed.* **2000**, *39*, 401.